Energy Transfer in Single-Stranded DNA-Templated Stacks of Naphthalene Chromophores

Amy L. Stevens,[†] Pim G. A. Janssen,[‡] Amparo Ruiz-Carretero,[‡] Mathieu Surin,[§] Albertus P. H. J. Schenning,[‡] and Laura M. Herz*,[†]

[†]Clarendon Laboratory, Parks Road, Oxford OX1 3PU, United Kingdom

[‡]Laboratory for Macromolecular and Organic Chemistry, Group Theoretical and Polymer Physics, and Institute for Complex Molecular Systems, Eindhoven University of Technology, Post Office Box 513, 5600 MB Eindhoven, The Netherlands

[§]Laboratory for Chemistry of Novel Materials, University of Mons, 20 Place du Parc B-7000 Mons, Belgium

S *Supporting Information*

ABSTRACT: We have investigated energy transfer in a novel self-assembled DNA hybrid structure composed of diaminopurine-equipped naphthalene derivatives that are hydrogen-bonded along a single-stranded oligothymine template. By performing time-resolved measurements of the naphthalene donor luminescence decay in the absence and presence of a cyanine Cy3.5 acceptor bonded covalently to the 5′ end of the oligothymine, we have examined the role of temperature and DNA template length on energy transfer from donors to the acceptor. We find that energy transfer rates decline with increasing temperature over a fairly narrow (± 5 °C) range over which changes in circular dichroism and donor luminescence lifetime indicate that the chiral assemblies are dissociating. In addition, the transfer rates exhibit a complex dependence on template length, increasing from initially low values for 10 bases toward an optimum for 30 bases and then declining again toward 60 bases. We find that for short ($\sim$10 bases) templates, incomplete filling and disorder reduces the overall transfer efficiency, while longer assemblies are more ordered but suffer from larger donor–acceptor separations, resulting in the observed peak at intermediate template length. In order to replicate the observed transfer dynamics, we have constructed a model assuming Förster energy transfer occurs between donors and acceptors whose geometric arrangement had been determined through molecular dynamics simulations of the whole assembly structure. For short DNA templates, the model is found to overestimate the transfer rates because it does not include effects of incomplete complex assembly and stacking faults. In contrast, the model underestimates the transfer rates for long, ordered assemblies indicating that additional mechanisms, such as diffusion of excitations along the donor stacks, need to be included. These results suggest that efficient energy transfer, in excess of that expected from simple Förster calculations, is feasible even for long DNA-templated assemblies of π-stacked conjugated chromophores. Such structures may therefore act as molecular wires transporting energy from one end to another.
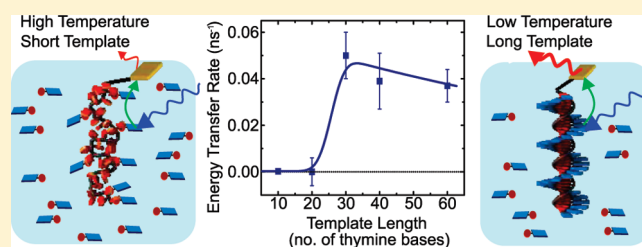
INTRODUCTION

Self-assembly, as pioneered by J. M. Lehn and others, has fast become a staple tool used in the control of complex supramolecular systems.[1−3] When governed by molecular recognition, self-assembly can produce systems with specific architectural and functional features determined by interactions of molecular components of the resulting aggregates.[4−6] The ensuant supramolecular systems are used as novel materials for devices or as model systems in which to study properties such as energy transport or the effect of disorder in a system. Typical interactions encountered in the supramolecular systems, such as hydrogen bonding, hydrophobic, hydrophilic, and $\pi−\pi$ interactions, are weak and highly temperature-dependent. Other important factors are steric constraints and cooperative binding, wherein the interaction of one molecule with a macromolecular system increases the affinity for binding other molecules to this system.[7] Self-assembly is a particularly attractive technique because of the ease of sample preparation from solution to a drop-casted film and the scope for up-scaling the technique to produce a large number of molecular nanostructures with well-defined morphologies.[8]

An additional aid in the design of self-assembled systems is the inclusion of a scaffold to fix the positions of the functional units, thereby aiding stability and reducing disorder, in these so-called "templated systems".[9] DNA is one example of a template found in nature as the formation of double-stranded DNA (dsDNA) is itself a cooperative self-assembly process.[10,11] Since the advent of DNA origami, where long DNA scaffold strands are folded into designer shapes with the help of short staple strands,[8,12] DNA has been used as a scaffold to form complex shapes[13] upon which nanoparticles and other materials may be bound with high

reproducibility.[14,15] DNA can act as a scaffold for assembly of pendant chromophores,[16] chromophores bound in the minor groove,[7] or chromophores incorporated between the bases in single-stranded DNA (ssDNA) before hybridization with the complementary ssDNA.[17,18] More generally, hydrogen bonding between specific nucleic bases has been utilized to form "DNA-like" self-assembled stacked structures.[19,20] These examples indicate that the properties of specific binding sites and of high monodispersity make DNA an attractive template upon which to bind chromophores. Chromophores that harness the specific bonding mechanisms to DNA can then be designed, such as multivalent guests that bond to DNA with high efficiencies.[21] This results in the synthesis of samples with specific packing orders that enhance the electronic and optical properties of a material.[22]

DNA-templated systems have been used in a multitude of ways, for example, as force sensors,[23] molecular beacons,[24] and molecular wires.[25,26] All of these applications rely on resonance energy transfer (RET) between luminescent dye molecules, and much effort has thus been devoted to understanding and improving such processes. For force sensors and molecular beacons, RET is detected in order to determine a change in distance between two dye molecules, a process that can be improved, for example, by using a dye—quencher pair that can form a ground-state complex[24,27] or by using a fluorescent base analogue such as 2-aminopurine[28,29] as one of the dye molecules. Molecular wires, on the other hand, are designed to allow energy to travel effectively between their ends—a process referred to as *energy transport*. Molecular wires are most commonly constructed from dsDNA to which dyes are either covalently bound,[25] intercalated between the nucleic bases,[26] or bound in the major or minor groove. However, efficiencies of energy transfer between the incorporated dyes are still limited by structural defects and varying conformations of the wire.[25] In addition, exact determination of the dye positions in the wires into which they are intercalated or groove-bound is still difficult, as the interchromophore distance is a function of the intercalator density.[26] Furthermore, intercalation by large dye molecules leads to local DNA-unwinding sites that can affect the structural integrity of the DNA.[26]

Since RET between self-assembled chromophores in a DNA scaffolded system is crucial to their use, an in-depth understanding of such transfer processes is of high importance. Most attempts at modeling the RET in such systems are based on the model originally developed by Förster[30] to describe the interactions between point dipoles associated with a randomly positioned small molecule forming part of a three-dimensional ensemble. However, the original Förster model clearly requires some modification in order to describe adequately DNA-scaffolded systems in which chromophores are in close proximity and in an ordered (quasi-1D) arrangement. One tentative way of including the effects of ordered geometry into Förster's original model is by adjusting the nominal dimensionality of the model used to describe the system.[31−34] In general, one can expect to observe an increased presence of short-lived and least-quenched donors for systems of lower dimensionality because of the increasingly effective excitation-energy trapping by nearest-neighbor chromophores.[34] However, an accurate description of the energy transfer requires the inclusion of a whole host of factors into the model, including the exact geometry of the assemblies, the shape of the chromphores, and the possibility of delocalization[35,36] and diffusion of excitations along the assembly.[37]

In this paper, we report a study of energy transfer in DNA-templated chromophore assemblies that overcome some of the difficulties of dye-intercalated DNA systems by employing direct hydrogen bonding of diaminopurine-equipped naphthalene derivatives to the bases of single DNA strands. This type of system has the advantage of allowing reversible positioning of the naphthalene chromophores along the DNA template into well-defined chiral assemblies in solution.[38] By choosing DNA templates with a single Cy3.5 acceptor dye covalently attached to one end, we investigated the energy transfer from randomly placed excitations on the DNA-bonded naphthalene assemblies to the assembly end. Using time-correlated single-photon counting (TCSPC), we were able to confirm the presence of energy transfer from naphthalene donors to Cy3.5 acceptors and investigate its dependence on temperature and DNA template length. We demonstrate that efficient energy transfer commences when the solution temperature is lowered and the naphthalene chromophores arrange into chiral aggregates. The rate of energy transfer extracted from the decay of the naphthalene-assembly luminescence in the presence and absence of the acceptor dye is shown to depend on the length of the DNA strands used as a template. When the number of base pairs in the DNA template is increased from 10, the transfer rate initially increases to peak at 30 base pairs and then decreases again toward 60 base pairs. These findings are commensurate with the cooperative assembly mechanism for templated assemblies: for short DNA templates, inefficient filling of the bases with naphthalene derivatives inhibits energy transfer. For longer DNA strands, on the other hand, the increase in transfer distances leads to a decrease in transfer rates, thus yielding an overall optimum in RET efficiency for 30 bases. In order to model the observed energy transfer rates, we have calculated the ensemble-averaged Förster energy transfer rates between the naphthalene donors and Cy3.5 acceptors based on assembly geometries extracted from molecular dynamics simulations of the DNA-templated structures. The model reproduces the experimentally observed trend of decreasing energy transfer rate for longer DNA templates. However, it underestimates the transfer rates for long assembly length, suggesting that additional transfer mechanisms, such as exciton diffusion along the assemblies, also need to be considered.

■ MATERIALS AND METHODS

The system under investigation self-assembles under the auspices of a collective of different chemical bonds as schematically shown in Figure 1. Blue bars represent the nonchiral diaminopurine—naphthalene derivative (NP) chromophores, whose synthesis has been detailed in ref 38 and in Supporting Information. The black strand represents the ssDNA template, denoted by Tn, which consists of n thymine bases. The most important interaction that drives template—NP binding is the triple hydrogen bonding of NP, via its diaminopurine end, to the pyrimidine unit of each thymine base. The hydrogen-bonding groups of these molecules are indicated by red bars in Figure 1. The synthetic design criteria and characterization for this and for a similar supramolecular system have been described in detail in refs 38 and 39 and refs 40 and 41, respectively. A complex range of intermolecular interactions influence the assembly process, which can be affected by even small changes in the molecular structure of the individual components.[41] Ethylene oxide side groups were selected for NP in order to allow solubility in water, while termination of the molecule with a hydroxy group was chosen to inhibit both NP aggregation and also further
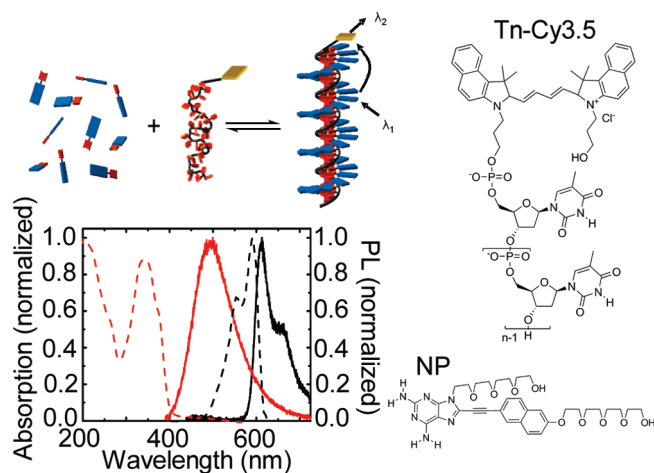
10551

dx.doi.org/10.1021/jp2036444 |*J. Phys. Chem. C* 2011, 115, 10550–10560

Figure 1. (Left, top) Schematic representing the self-assembly of diaminopurine—naphthalene derivatives (NP) along a single-stranded oligothymine template. Samples were prepared in ultrapure water with an NP concentration of 1.6 mM and an oligothymine template concentration that corresponded to a thymine base concentration of 0.4 mM. The final structure obtained has a right-handed helical nature at low (≤20 °C) temperatures. (Left, bottom) UV—vis absorption and photoluminescence spectra for the NP donor (red dashed and solid lines, respectively) and the Cy3.5 acceptor when attached to a 20-base oligothymine (black dashed and solid lines, respectively). (Right) Chemical structures of NP and cyanine dye Cy3.5 bonded to the 5′ end of the oligothymine.

aggregation of the whole DNA hybrid complex.[40−42] In addition, the NP donor was designed specifically to incorporate a diaminopurine hydrogen-bonding unit, because the diaminopurine's large π-conjugation area strengthens the donor—donor interactions that should promote stabilization of the assembly, especially for long template lengths.[38]

Previous characterization of these assembled systems has revealed that the hydrogen bonding of NP to the template is weaker than bonds between complementary bases in dsDNA and highly specific.[38] NPs did not bind to strands of adenine or cytosine bases, and dsDNA was formed in preference to retention of the NP—oligothymine aggregates when a strand of complementary adenine bases was added to solutions containing the templated assembly.[38,42] Molecular modeling and morphological studies show that the stacking geometry and resulting chiral order strongly depends on the nature of the chromophore. For naphthalene-based systems, the relatively weak interactions between such molecules yield assembled supramolecules resembling the dsDNA B-helix structure.[43] A simple one-dimensional Ising model has been used to demonstrate that the interplay between the energies involved in donor—oligothymine (guest—host) and donor—donor (guest—guest) binding has a strong influence on the formation of the aggregates.[41] Spectroscopic evidence for the formation of templated assemblies has also been presented: upon mixing the donor with the template, the absorption band was found to be blue-shifted and mitigated in intensity, while the circular dichroism spectrum exhibited a positive Cotton effect in the naphthalene absorption region.[38] These results are indicative of the formation of chiral aggregates,[18] with the oligothymine template inducing a right-handed helical structure as NP binds to it. The length and thickness of 20-base templated assemblies, containing diaminotriazine hydrogen-bonding naphthalenes, have been determined

to be approximately 7 nm and 3.5−4 nm, respectively, based on a combination of cryo-transmission electron microscopy (cryo-TEM), angle-dependent dynamic light scattering (DLS), atomic force microscopy (AFM), and molecular dynamical modeling.[41,43]

To permit investigations of energy transfer in the DNA-templated assemblies, an acceptor Cy3.5 cyanine dye (yellow bar in Figure 1) was covalently bonded to the phosphate group at the 5′ end of the ssDNA. Cyanine dyes are characterized by two heterocyclic components connected by a polymethine bridge. They offer large extinction coefficients, moderate fluorescence quantum yields, and widespread applicability as photosensitizers, stains, and fluorescent probes.[7] The absorption and photoluminescence spectra shown in Figure 1 display a cyanine dye absorption peak at 589 nm and an emission peak at 612 nm. For NP, absorption is found to peak at 344 nm and emission broadly around 480 nm. The spectral overlap between the NP donor chromophore emission and the Cy3.5 acceptor absorption should thus permit efficient energy transfer from the former to the latter chromophore.

In order to assess the dependence of energy transfer on the assembly length, we used samples containing oligothymines with different numbers of bases n ($n = 10, 20, 30, 40$, or 60). To allow accurate relative measurement, we prepared a complex (NP-Tn-Cy3.5), an acceptor (Tn-Cy3.5), and a donor (NP-Tn) sample for each oligothymine length. Here, the acceptor sample comprised a Cy3.5 acceptor dye covalently bonded to the 5′ end of the n-base oligothymine; the donor sample, an n-base oligothymine template decorated with NP donors; and the complex sample, a Cy3.5 dye bonded to the donor-decorated n-base oligothymine template. Samples were prepared in ultrapure water with an NP concentration of 1.6 mM and an oligothymine template concentration that corresponded to a thymine base concentration of 0.4 mM. Therefore, each base site was available to an average of four NP in order to promote filling of the template binding sites at low temperatures.[38] In the absence of the template, NP is dissolved molecularly at this solution concentration; that is aggregation effects should not be expected.[38]

We conducted time-correlated single-photon counting (TCSPC) measurements on the DNA-hybrid samples using Becker & Hickl SPC-130 TCSPC electronics. During the measurements, the sample solutions were held in microcuvettes mounted on a temperature-controlled stage that allowed temperature adjustments between 15 and 90 °C with an accuracy of 1 °C. The samples were excited at 375 nm with an excitation power of 30 μW by use of the frequency-doubled pulsed output from a Ti:sapphire Tsunami laser with 82 MHz repetition rate. The photoluminescence (PL) emerging from the sample was collected by two off-axis parabolic mirrors along a trajectory orthogonal to the excitation. The PL was then dispersed in a monochromator and directed onto a Peltier cooled photomultiplier tube, yielding an overall time resolution of 180 ps. We chose the excitation wavelength to excite predominantly the NPs, and we set the excitation power and collection time (25 s per TCSPC scan) so that sample degradation was reduced to an acceptable minimum. In addition, the low excitation powers and high pulse repetition rate mean that measurements were taken in a linear regime, with significantly fewer than one excitation placed per assembly at any given time. Time-integrated photoluminescence (TIPL) measurements were carried out by imaging the monochromator-dispersed PL on a nitrogen-cooled charge-
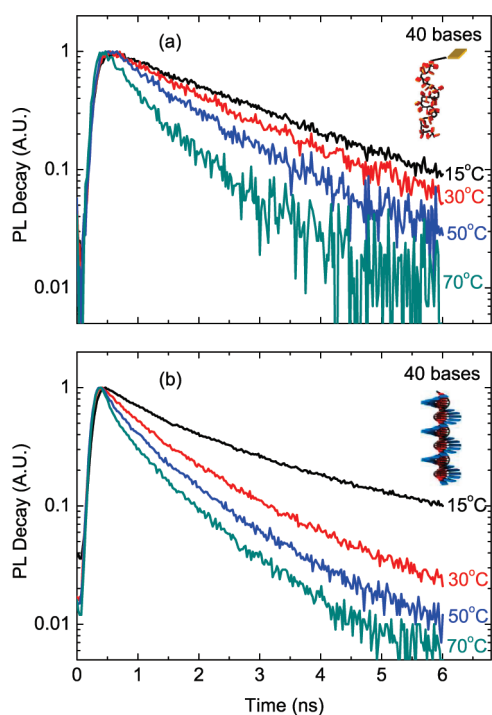
Figure 2. (a) Time-resolved photoluminescence of Cy3.5 attached to 40-base oligothymine (acceptor) for different temperatures, detected at the peak (620 nm) of the emission spectrum. (b) PL decay of a 40-base oligothymine—NP assembly lacking the Cy3.5 dye (donor) for different temperatures, detected near the peak (507 nm) of the emission spectrum.

Figure 3. PL decay lifetimes for (a) acceptor (T40—Cy3.5) and (b) donor (NP—T40) as a function of temperature, extracted from the PL decay curves shown in Figure 2 by fitting a monoexponential function to the data within the range 0.4 ns (TCSPC peak) to 6 ns (T40—Cy3.5) or 1.5—5 ns (NP—T40). Solid lines are guides to the eye.

coupled device. The TIPL spectra were corrected for the spectral response of the apparatus by use of a calibrated filament lamp. When not in use for short durations, the samples were stored in a darkened environment in air at room temperature; they were stored in a freezer at other times.

■ RESULTS AND DISCUSSION

Our previously published measurements[38] of circular dichroism (CD) for NP-Tn assemblies have demonstrated that the intensity of the Cotton bisignate signal decreases with increasing solution temperature. Since the CD signal is caused by the interaction between NP chromophores arranged in a chiral assembly, these data suggest that ordered attachment to the template will commence for the samples investigated here when the temperature is lowered below ~25—30 °C. In addition, the amount of ordered assembly was strongly dependent on template length: monitoring the CD signal at the NP absorption peak (354 nm) at a constant low temperature revealed that the signal was strongest for long templates and near zero for the shorter templates ($n \sim 10$ bases).[38]

We performed initial measurements of TIPL spectra (not shown) for donor, acceptor, and complex samples and observed relative donor peak quenching and acceptor peak enhancing for the complexes at low temperatures, in qualitative agreement with energy transfer between Cy3.5 and NP when integrated in the complex. All TIPL peak heights recovered fully when the samples were cycled thermally between 15 and 70 °C, confirming that supramolecular assembly is a reversible process for this system. A slight red shift with decreasing temperature was identified for the
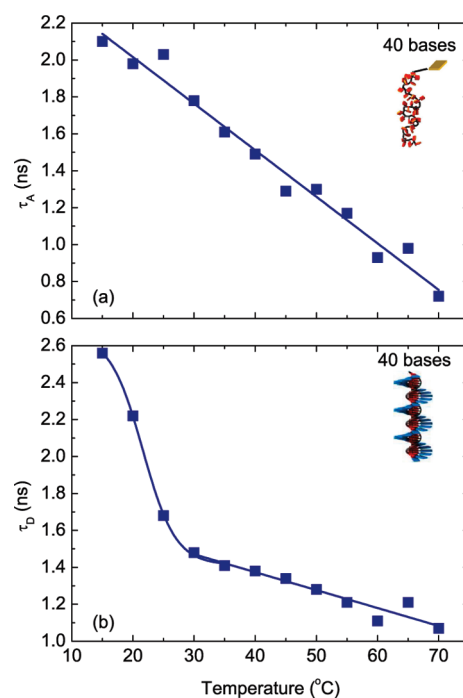
donor peak, in accordance with aggregation[44] of the NPs, induced by the oligothymine template at low temperatures. In addition, the measurements showed that both the donor and acceptor peak intensities decreased with increasing temperature, which complicates a quantitative assessment of energy transfer based on such data alone. We therefore instead base our following analysis on measurements of the time-resolved emission recorded for the donor, acceptor, and complex samples.

Donor and Acceptor Decay Dynamics. For an accurate assessment of energy transfer in the DNA-templated complexes, we first measured and analyzed the PL decay dynamics of the donor and the acceptor in the absence of other species. To investigate the effect of temperature on the lifetimes of the donor (NP-Tn) and acceptor (Tn-Cy3.5) samples, we performed TCSPC measurements for n = 40 for a range of different temperatures. Figure 2 shows the normalized PL decays of (a) the acceptor sample, detected at 620 nm, and (b) the donor sample, detected at 507 nm. While the acceptor PL decay is monoexponential, the donor PL is slightly nonexponential, concomitant with the presence of both aggregated NP on the template and excess molecularly dissolved NP. Both species show faster PL decay with increasing temperature. To quantify the changes in lifetimes, these data were fitted with single exponentials, and the resulting lifetimes are displayed in Figure 3 as a function of temperature for both the acceptor (τ_A) and the donor (τ_D).

Figure 3a indicates that the lifetime of Cy3.5 bound to the DNA template decreases almost linearly from its value of 2.1 ns at 15 °C to 0.7 ns at 70 °C, suggesting increasingly efficient nonradiative excitation pathways at higher temperatures. It is not thermodynamically favorable for the dye to be quenched via photoinduced electron transfer by the thymine bases of the
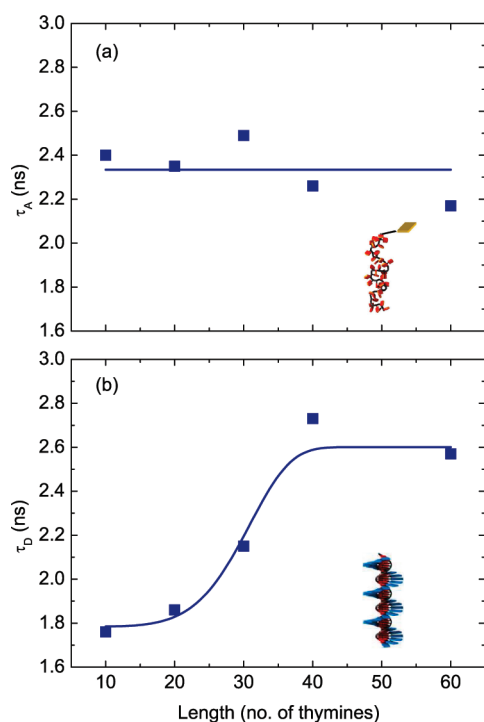
Figure 4. (a) Acceptor (Tn–Cy3.5) and (b) donor (NP–Tn) lifetimes for different oligothymine lengths n, extracted through monoexponential fitting to the PL decays measured at 15 °C at the emission peak wavelengths. Solid lines are guides to the eye.

Figure 5. Photoluminescence decay of acceptor (T60–Cy3.5) and complex (NP–T60–Cy3.5) samples, measured at 620 nm for (a) low (15 °C) and (b) high (50 °C) temperature. At 50 °C, the complex has dissociated with the donors molecularly dissolved in solution.

template,[45,46] as shown in a study of the relative excited-state reduction potential of a Cy3 dye and oxidation potentials of various nucleobases.[47] Collisions with solvent molecules and intramolecular vibrations may make a contribution to such effects. However, the observed trend is most likely caused by changes in photoisomerization which has been shown to provide an efficient nonradiative deactivation pathway for cyanine dyes, especially those with short polymethine chains.[46] In this process, the polymethine linkers adopt an all-trans configuration in solution until, upon absorption of light, the dyes isomerize from the first excited singlet state to a ground-state photoisomer that adopts a mono cis conformation.[46] The isomerization occurs via a partially twisted intermediate excited state. The cis photo-isomer undergoes a thermal back-isomerization to yield the ground-state trans isomer.[48] Attaching a cyanine dye to a bulky substituent, such as a long oligothymine molecule, increases the activation energy of isomerization, thus increasing the lifetime of the dye.[46] Comparable effects have been noted for the similar dye Cy3, which in solution has a lifetime of ~0.2 ns that increases to ~2 ns when it is attached to ssDNA.[46,49] Isomerization is an activated process that depends strongly on the temperature of the medium such that a decrease in lifetime with temperature, as shown in Figure 3a, is to be expected.

Figure 3b shows the temperature dependence of the NP donor lifetime τ_D, which exhibits a sharp decrease between 15 and 30 °C superimposed on a more subtle linear decrease toward higher temperature. The lifetime of aggregated NP is longer than that for unbound NP; therefore the initial sharp decrease of τ_D indicates the detachment of NP from the oligothymine once the complex dissolves around the transition temperature. These trends in donor lifetimes are matched by those found in circular
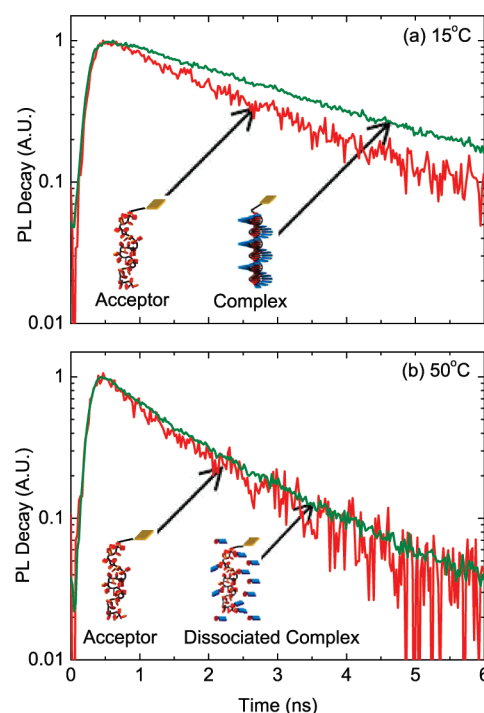
dichroism (CD) measurements (vide infra): as the temperature is raised above ~25–30 °C, the CD signal disappears in accordance with the dissolution of helical aggregates of NP, as previously observed in similar complexes.[41] The small, linear decrease of donor lifetime with temperature is likely to be again caused by an increasingly efficient nonradiative pathway, possibly involving the solvent and relaxation of vibrational states.

We determined the dependence of the acceptor and donor lifetimes (at 15 °C) on oligothymine template length using the same procedure as described above. The results are displayed in Figure 4, which indicates that the acceptor has a length-independent lifetime with an average of 2.33 ns. This is in excellent agreement with the value of 2.31 ns reported for a Cy3.5 dye attached to ssDNA consisting of approximately 30 bases.[24] The donor lifetime, on the other hand, increases from ~1.8 ns for short ($n = 10$) oligothymines to ~2.6 ns for long ($n \geq 40$) oligothymines. As already mentioned, the donor lifetime depends on the degree of templated assembly of NP and, hence, the ordering and distribution of the NPs on the template. On short templates, similar naphthalene derivatives have been shown to be arranged in a disordered assembly with varying distances between conjugated units along the template.[43] CD spectra corroborate this theory as smaller templates exhibit low peak intensities (vide infra), showing that the donors barely bind to the 10-base oligothymine, thus decreasing the donor PL lifetime. The cooperative nature of the assembly means that a minimum template size is clearly needed to stabilize the hybrid complex.[38] There is theoretical evidence that, at low temperatures, short templates in solution are either filled with similar naphthalene derivatives or empty. Mixed forms are not favored because of a lack of combinatorial entropy as fewer mutually distinguishable distributions of bound guest molecules are possible.[41] In contrast, temperature-dependent UV absorption experiments for similar DNA-templated complexes
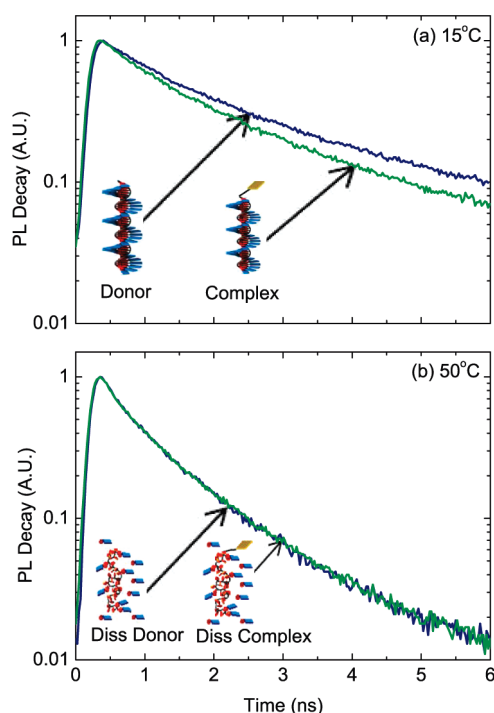
Figure 6. Photoluminescence decay of donor (NP−T60) and complex (NP−T60−Cy3.5) samples, measured at 507 nm for (a) low (15 °C) and (b) high (50 °C) temperature. At high temperatures, the donor and complex samples have dissociated (labeled diss donor and diss complex, respectively); see the text for details.

show that stronger guest−guest interactions exist for longer templates, which increases the stability of the stack and the ordering of the donors along the template.[41] It is important to note that the diaminopurine−naphthalene derivative donors used in this study have a stronger guest−guest interaction energy and a weaker host−guest interaction energy than the similar diaminotriazine−naphthalene derivatives referred to above.[38] Hence, it can be assumed that the donor arrangement on short templates is disordered and that the donors may have limited binding to short templates.

Energy Transfer Dynamics in Donor−Acceptor Complexes. In order to assess the rate at which energy transfer occurred between naphthalene and Cy3.5 chromophores, we proceeded to measure (A) the Cy3.5 PL decay on the template with and without NP attached (i.e., for acceptor vs complex samples), and (B) the NP luminescence decay on the template with and without Cy3.5 attached (i.e., for donor vs complex samples) for all template lengths. Figure 5 shows an example of such data for the 60-base oligothymine for case A at two different temperatures, 15 and 50 °C, at which the complexes are respectively either assembled or fully molecularly dissolved. At low temperature, the Cy3.5 luminescence is longer-lived when NP is present, suggesting energy transfer from NP to Cy3.5 occurs. However, this discrepancy is not fully removed when the complexes are dissociated at 50 °C. It is unlikely that significant energy transfer occurs from dissociated NP to the Cy3.5 dyes at the low solution concentrations employed. Instead, the higher viscosity of the complex solution caused by the presence of NP may induce interactions that affect the photoisomerization of the dye[50] and hence modify the Cy3.5 lifetime.

Figure 6 shows the peak-normalized PL decay for NP donors in the presence of the 60-base oligothymine template with and without the covalently bonded acceptor dye (case B) at 15 and 50 °C. These data demonstrate that the lifetime of the donors is shorter in the presence than in the absence of Cy3.5 acceptors. This difference disappears when the solution temperature is raised beyond the point at which the complexes dissociate. Both the lengthening of the acceptor lifetime in the presence of donors and the shortening of the donor lifetime in the presence of acceptors, over the same time scale, provide strong evidence for the occurrence of energy transfer between the donor and the acceptor when complexes form at low temperatures. In order to obtain more quantitative information on the transfer rates involved, we proceeded to analyze the changes in NP luminescence in the presence and absence of Cy3.5 (case B) to avoid complications caused by direct acceptor excitation and solution viscosity changes affecting the acceptor lifetime, as mentioned above.

Energy transfer in π-conjugated donor−acceptor systems generally relies on electric-dipole coupling between the emitting transition moment of the donor and the absorptive transition moment of the acceptor. Based on the weak coupling limit of radiationless transitions, Förster[30] derived the rate constant for the transfer process involving a single donor−acceptor pair to be

$$K_{D^* \to A^*} = \frac{1}{\tau_D} \left(\frac{R_0}{R} \right)^6 \tag{1}$$

where τ_D is the mean lifetime of the excited donor, R_0 is the critical transfer distance for which excitation transfer and spontaneous deactivation are of equal probability, and R is the distance between donor and acceptor species.[30,51] Equation 1 implies that the transfer rate is independent of exciting wavelength and is thus valid only if the donor molecule is in the lowest vibrational level of its excited state.[52] For an ensemble of randomly distributed chromophores, a range of acceptor−donor distances will be present in the material, requiring an ensemble average to be determined that will depend on the geometry of the system.[32] Furthermore, the size of the molecules is restricted to being smaller than intermolecular separations when such point-dipole models are used to calculate the electronic coupling that promotes energy transfer from one molecule to another.[32,52]

The additional decay path induced by Förster RET for donor excitons must be considered when the de-excitation of the donor through all mechanisms is described.[31,34,53] In the absence of acceptors, the time-dependent PL decay of the donor bound to the template can be described by

$$I_D(t) = \hat{I}_D \exp \left(\frac{-t}{\tau_D(t)} \right) \tag{2}$$

where $\hat{I}_D$ is the intensity at time $t = 0$ and τ_D is the donor ensemble lifetime, which may be time-dependent. In the presence of acceptors, the time-dependent PL decay of the donor is given by

$$I_C(t) = \hat{I}_C \exp \left[-t \left(\frac{1}{\tau_D(t)} \right) + k_{ET}(t) \right] \tag{3}$$

where $\hat{I}_C$ is the complexes' PL intensity at $t = 0$ and $k_{ET}(t)$ is the energy transfer rate to the acceptors. However, as mentioned above, an excess of three donors per DNA binding site was added in order to ensure that the sites are more likely to be filled effectively.[38] In order to obtain I_D and I_C from the measured data, we therefore first carefully removed the PL background arising from the presence of the unbound donors, which was facilitated
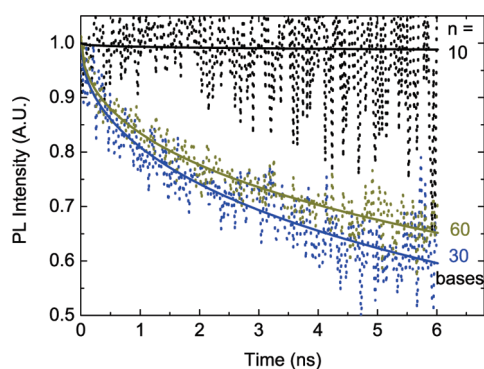
Figure 7. Energy transfer dynamics reflecting the NP emission decay arising solely from energy transfer to Cy3.5. The curves are derived from the donor PL transient, of which some are shown in Figure 6, by removing the contribution arising from excess unattached NP and from intrinsic donor excitation decay, as described in the text. Solid lines are fits to the data by use of the stretched-exponential function given by eq 5.

by taking into account that at temperatures over 50 °C all NP molecules are not hydrogen-bonded to the template. We thus subtracted from the low-temperature (15 °C) PL curves the fraction of the high-temperature (50 °C) curves corresponding to the donor excess and thereby obtained the PL decay contribution attributable only to the donors bound into complexes (for a more detailed description, see Supporting Information). We then proceeded by dividing the obtained donor PL decay of the complexes by the donor PL decays in the absence of acceptors:

$$I_{ET}(t) \equiv \frac{I_C}{I_D} = \hat{I}_{ET} \exp[-tk_{ET}(t)] \qquad (4)$$

These final obtained decay curves I_{ET} reflect *solely* the decay of excitation placed on NP molecules forming part of a complex with the *only* cause for donor de-excitation being energy transfer to acceptors.[53]

Figure 7 shows the extracted energy transfer dynamics I_{ET} for complexes formed at 15 °C for a number of different template lengths. We find that the transfer dynamics accelerate from complexes with template length of $n = 10$ base pairs toward those with $n = 30$ bases, for which they are fastest, and then reduce again toward complexes with $n = 60$ bases. In addition, we find that the shape of the curves can be described in all cases by a stretched exponential:

$$I_{ET}(t) = \hat{I}_{ET} \exp\left[-\left(\frac{t}{\tau_0}\right)^d\right] \qquad (5)$$

Comparison with eq 4 yields an energy transfer rate $k_{ET} = t^{d-1}\tau_0^{-d}$, where τ_0 and d are time constants affecting the time-dependent rate of energy transfer k_{ET}. Such time-dependent energy transfer rates are very commonly observed for complex systems[32,53,54] and may arise from a multitude of causes, such as exciton diffusion or inhomogeneous chromophore arrangement in the system. When acceptors are randomly distributed throughout an arrangement of donors, the energy transfer dynamics have been shown to adopt the stretched-exponential behavior[32] described by eq 5 because of the range of donor—acceptor distances present. In this case, the exponent d directly relates to the dimensionality Δ of the system,[55,56] with $\Delta = 6d$. For such systems, decreasing dimensionality for fixed acceptor concentrations leads to an increasing
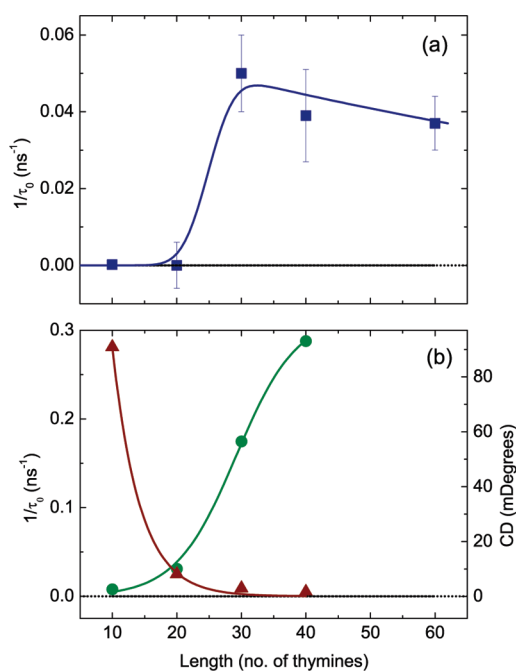

Figure 8. (a) Energy transfer rate constant τ_0^{-1} extracted from stretched-exponential fits to the energy transfer dynamics shown in Figure 7, plotted as a function of the number n of oligothymine bases forming the template. (b) (●, green) Circular dichroism signal at 354 nm as a function of oligothymine length n at 15 °C. (▲, maroon) Values for the energy transfer rate constant extracted from a model based on Förster energy transfer in complexes whose structure had been determined through molecular dynamics simulations, as described in the text. The rate constant was obtained by fitting stretched exponentials to the simulated energy transfer dynamics and is plotted as a function of oligothymine length. The solid lines are guides to the eye.

emphasis of fast initial PL decay as well as very slow PL decay components, a behavior attributed to the increasing dominance of nearest neighbors in the trapping of excitation energy.[34,54] We have fitted eq 5 to the energy transfer curves as in Figure 7, and we find that, for all temperatures and template lengths for which stable assemblies form, $d = 0.6 \pm 0.1$. This value suggests a "dimensionality" of $\Delta = 3.6 \pm 0.6$. However, for the DNA-templated system under investigation here, the constant d cannot be directly linked with system dimensionality, as the acceptor chromophores are not randomly distributed but attached solely to the end of a strand of donors. As detailed in the next section, we therefore developed a model that incorporates a realistic structure of the complexes. The value of energy transfer rate constant τ_0^{-1} was also extracted for the value of $d = 0.6$ and is displayed in Figure 8a as a function of DNA template length.

τ_0^{-1} is found to be strongly template-dependent: it is initially low for short oligothymines and rises with an increase in the length of the oligothymine template, then peaks for the 30-thymine strand with $\tau_0^{-1} \sim 0.05$ ns^{-1}, and subsequently decays toward longer (≥ 60) template lengths. This complex behavior arises from the contributions of two counteracting effects. For short templates, incomplete attachment of NP to the template suppresses the energy transfer,[38] while for long templates, an increase in donor—acceptor distances also leads to a reduction. Therefore, an overall maximum in transfer efficiency can be expected for a particular template length. Figure 8b shows the CD amplitude measured for complex samples of different lengths
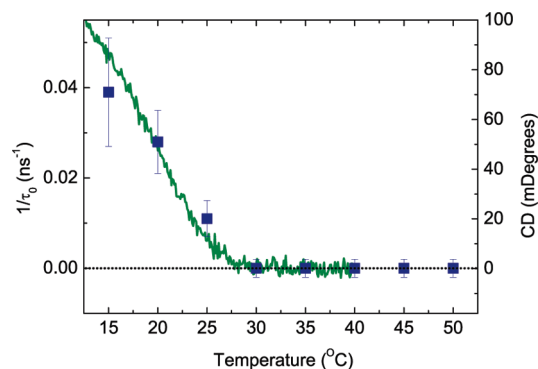
Figure 9. (■, blue) Experimentally determined energy transfer rate constant (τ_0^{-1}) extracted from fits of a stretched exponential (eq 5) to the energy transfer dynamics for a 40-base oligothymine (see Figure 7), as a function of temperature. The green solid line is the circular dichroism signal measured at 354 nm as a function of temperature.

(NP−Tn−Cy3.5), at 15 °C and a detection wavelength of 358 nm, near the peak of the donor absorption. A sharp onset in the CD amplitude arising from the Cotton effect can be clearly seen at $n \sim 20-30$, matching the similar rise in energy transfer rate constant over that range. As discussed in the following section, we have also extracted values for τ_0^{-1} from a model based on the geometric arrangement of the chromophores in the complexes under study. Figure 8b also shows these theoretical values for τ_0^{-1}, which decline sharply for template lengths $n \geq 10-20$. The resulting interplay between completeness of assembly and donor−acceptor separation thus leads to the observed peak in energy transfer rates around $n \sim 30$ in these systems.

In addition, we investigated the influence of solution temperature on the energy transfer by extracting the transfer dynamics, correcting as described above for excess donor and intrinsic donor PL, for the 40-base oligothymine sample. The resulting decay curves were again fitted with eq 5 for $d = 0.6$, and the resulting τ_0^{-1} values are displayed in Figure 9 as a function of temperature. The energy transfer rate parameter shows a strong correlation with the CD amplitude measured for the same complexes. As the system becomes more disordered at high temperatures and finally dissociates, the transfer rate constant τ_0^{-1} tends to zero.

Simulation of Energy Transfer in the Complexes. We have carried out simulations of Förster energy transfer from individual NP donors to Cy3.5 acceptors using geometry-optimized structures of the DNA-templated assemblies extracted from molecular modeling. These calculations were carried out on systems made of 10−40 oligomer donors, each being hydrogen-bonded to a thymine base of a single-stranded DNA. The single-stranded DNA was end-capped with the cyanine-based molecule Cy3.5 covalently bonded to the final phosphate group. The starting structures of both guest and dye were built in extended conformation. The ssDNA structure was constructed in the canonical B-helix structure with sodium (Na$^+$) counterions along the phosphate backbone and the stack of guests was built in Watson−Crick base pairing, following the simulations described in ref 43 Molecular dynamics simulations were carried out with the CHARMM force field in the canonical ensemble at 288 K (Berendsen thermostat) in implicit solvent model on a 10 ns time scale with a 1 fs time step. Figure 10 shows a geometry-optimized starting conformation for the 10-base complex, which has been used to construct longer assemblies and model the transfer rates (see Supporting Information).
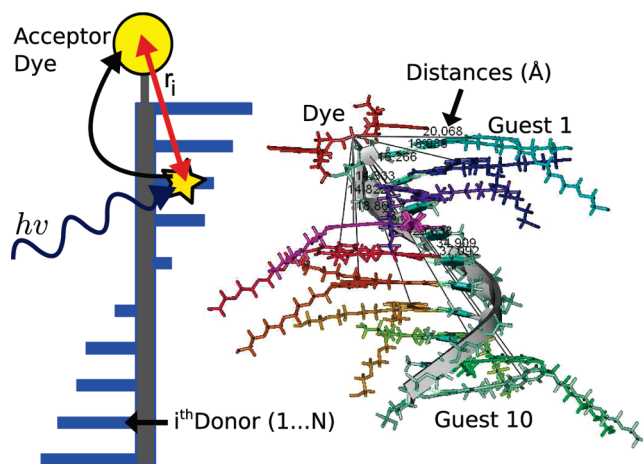

Figure 10. (Left) Schematic depiction of the approach used in the model describing Förster resonance energy transfer in the DNA-templated complexes. The gray strip is the oligothymine template, each blue rectangle represents an NP donor, and the yellow circle is the acceptor Cy3.5 dye. Random excitation of an NP chromophore is followed by possible energy transfer to the Cy3.5 dye positioned at the DNA end. (Right) Example of a geometry-optimized structure for the 10-base DNA assemblies extracted from molecular simulations, as described in the text. Counterions are not shown for the sake of clarity. The geometries obtained for the systems were used to extract the distances r_i between the ith NP chromophore and the Cy3.5 dye center, which were used for calculation of the individual transfer rates.

In order to describe the dynamics of donor de-excitation resulting from energy transfer *only*, we need to calculate the total emission intensity I_{total} by summing over the individual contributions $I_i(t)$ from each NP donor on the template:

$$I_{total}(t) = \frac{1}{N} \sum_{i=1}^{N} I_i(t) \tag{6}$$

For each individual donor i, the energy transfer rate is given by eq 1 with the individual donor−acceptor distances r_i being defined as the distance from the center of the Cy3.5 acceptor electronic transition dipole to the center of the naphthalene chromophore transition dipole contained in each donor:

$$I_{total}(t) = \frac{I_0}{N} \sum_{i=1}^{N} \exp\left[-\frac{t}{\tau_D^{rad}}\left(\frac{R_{0,i}}{r_i}\right)^6\right] \tag{7}$$

Here, τ_D^{rad} is the intrinsic or *radiative* lifetime of donors in the absence of acceptors, and $R_{0,i}$ is the distance at which energy transfer between the ith donor and the acceptor is as likely to occur as *radiative* recombination of the donor exciton.[30] The radiative Förster radius $R_{0,i}$ for each donor i was calculated from[30]

$$R_{0,i} = \left[\frac{9000 \ln 10}{128\pi^5} \frac{\kappa_i^2}{n^4 N} \int_0^\infty \frac{1}{\bar{\nu}4} f_D(\bar{\nu}) \varepsilon_A(\bar{\nu}) \, d\bar{\nu}\right]^{1/6} = \rho_0 \kappa_i^{1/3} \tag{8}$$

Here, κ_i^2 is the dipole orientation constant for the ith donor with respect to the acceptor, n is the refractive index of the material at the peak of the integrand, N is Avogadro's constant, $f_D(\bar{\nu})$ is the fluorescence spectrum of the bound NP donor with integrated intensity normalized to unity on a wavenumber scale, and $\varepsilon_A(\bar{\nu})$ is the molar decadic extinction coefficient of the acceptor
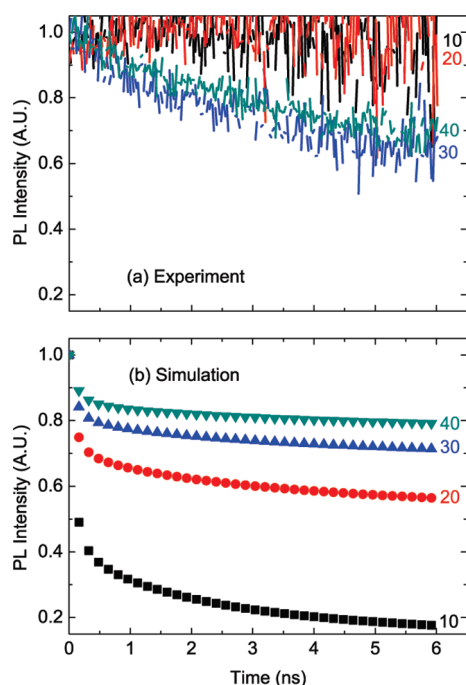
10557

dx.doi.org/10.1021/jp2036444 |*J. Phys. Chem. C* 2011, 115, 10550–10560

Figure 11. (a) Experimental and (b) calculated energy transfer dynamics for complexes containing oligothymine templates of lengths ranging from 10 to 40 bases. The calculated curves were extracted from a model based on donor−acceptor distances obtained from the geometrically optimized structure of the assemblies shown in Figure 10.

Table 1. Experimental and Theoretical Energy Transfer Rate Constants[a]

no. of thymines	$\tau_{0,\text{exp}}^{-1}$ (ns^{-1})	$\tau_{0,\text{calc}}^{-1}$ (ns^{-1})
10	$<10^{-3}$	0.281
20	$<10^{-3}$	0.025
30	0.050	0.009
40	0.039	0.005

[a] Obtained upon fitting eq 5 to the energy transfer dynamics shown in Figure 11.

hydrophobic and attractive electrostatic forces,[7,57] and $\pi-\pi$ stacking, especially for purine bases.[45] Hence, we calculate a separate κ_i^2 value for each donor−acceptor pair such that the specific geometric arrangement for each naphthalene donor dipole and the acceptor dipole pair is preserved:

$$\kappa_i^2 = [\hat{a} \cdot \hat{d}_i - 3(\hat{a} \cdot \hat{r}_i)(\hat{d}_i \cdot \hat{r}_i)]^2 \qquad (9)$$

Here, $\hat{a}$ and $\hat{d}_i$ are unit vectors in the direction of the acceptor and ith donor transition dipoles, respectively, and $\hat{r}_i = \vec{r}_i / r_i$ is the unit vector in the direction connecting the center of the acceptor dipole and the center of the ith donor dipole, where $r_i = \|\vec{r}\|$ is the donor−acceptor dipole separation as used in eq 7. These vectors are determined by using atom positions, relative to a common origin, in the geometry-optimized 40-donor complex from molecular simulations (see Supporting Information). Figure 10 shows as an example the calculated structure for a shorter 10-unit complex for ease of viewing. Thus, the calculated κ_i^2 values obtained from this procedure reflect the real structure of the complexes.

τ_D^{rad} was calculated from the experimentally determined lifetime τ_D of the excited donor by use of $\tau_D = \eta_D \tau_D^{\text{rad}}$, where η_D is the quantum yield of the bound NP donors (see Supporting Information). Equation 7 realistically assumes that each NP on the template has, on average, the same probability of being excited. Subsequently, energy transfer causes a decay in the excited-NP ensemble population, which leads to a nonrandom distribution as donors close to the acceptor transfer their excitation faster than those further away. The ensemble transfer rate thus decreases with increasing time after excitation, as only those excitations survive that are located far from acceptors.[51,53] Hence, these effects cause a time dependence in the ensemble transfer rate, as observed experimentally for these samples.

In order to obtain the simulated energy transfer dynamics for the donor, eq 7 was evaluated at 0.02 ns intervals between 0 and 6 ns, by use of donor−acceptor distances derived from the $\vec{r}_i$ vectors and κ_i^2 values evaluated from eq 9 (see Supporting Information for a table of $\|\vec{r}\|$ and κ_i^2 values). Donor de-excitation curves were calculated for template lengths n ranging between 10 and 40 with corresponding τ_D^{rad} values of 1.95−3.03 ns. The resulting curves are displayed in Figure 11b together with the experimental data (Figure 11a). The calculated curves again show stretched-exponential behavior; however, they appear to show a much more pronounced dependence on template length than the experimental curves. To allow comparison of numerical values, we also fitted eq 5, with $d = 0.6$, to the simulated donor decay curves. The values extracted for the energy transfer rate constants, τ_0^{-1}, are given in Table 1 together with those previously determined from experimental data.

Table 1 and Figure 11 clearly show that the calculated transfer rate, $\tau_{0,\text{calc}}^{-1}$, overestimates the experimental transfer rate, $\tau_{0,\text{exp}}^{-1}$, for the shortest template length and underestimates it

$(1.5 \times 10^3 \text{ L·mol}^{-1}\text{·cm}^{-1}$ at the peak of the spectrum).[30,51] The integral depending on donor emission and acceptor absorption was determined by discrete summation over the experimental data products and also (in order to estimate the errors born of this method) by numerical integration of functions fitted to the donor and acceptor spectra, which yielded very similar results. The refractive index n was taken to be 1.33, that of bulk water, as done previously for the case of fluorescein.[57] Inserting these values into eq 8 yields a value of $\rho_0 = 31 \pm 1$ Å.

κ_i^2 is related to the relative orientation of the acceptor absorption and ith-donor emission transition moments. The lowest-energy singlet absorption and emission transitions in naphthalene are polarized along the long axis of the molecule, a ^1L_b state in Pariser notation.[58] This was established in the late 1950s[59−63] and has been supported by more recent experimental[64] and theoretical investigations.[65,66] For cyanine dyes, the $\pi-\pi^*$ transition moment lies along the in-plane long axis of the molecule defined by the polymethyne chain.[49,50,67−69] If the donor or acceptor reorients rapidly within the lifetime of its excited states, then the value of κ^2 for this system is $^2/_3$; otherwise, a range of values are obtained depending on the relative donor−acceptor pair orientation.[51,70] Several past studies on systems with cyanine dyes attached to ss- or ds-DNA via a flexible 3- or 6-carbon tether have explored the attachment mode of these dyes. Experiments have probed the activation energies of the isomerization of free and tethered cyanine dyes,[48,71] the anisotropy of tethered dyes,[46,57,69] and the modulation of FRET efficiencies after varying the number of base pairs between cyanine dyes attached to opposite ends of a DNA helix.[49] The emerging consensus is that cyanine dyes stack rigidly across the terminal base pair of the DNA similar to the way an additional base pair would.[67] The dye is held in position by a combination of

for the longer template lengths. The former is understandable as the model does not take into account the effect of disorder, due to poorly formed assemblies, slowing energy transfer in the assemblies, and hence $\tau_{0,\text{calc}}^{-1}$ is too high in particular for the shorter (10−20 base) templates, for which such effects are strong. However, one would expect experimental and simulated values to converge for long template lengths, for which the assemblies are expected to be fully formed and well-ordered.[38] The point-dipole approximation incorporated into the Förster model may be inappropriate for the fraction of donor molecules very near the acceptor molecule, as the donor−acceptor distances here become comparable to the extent of the excitations themselves.[52,72] However, such effects are likely to be insignificant for the longer (40-base) templates, for which most donors are far from the acceptor. Bimolecular processes such as exciton−exciton annihilation have been shown to have an effect on excitation transfer dynamics;[73] however, the low laser fluence used to excite the samples in our study means that such processes are highly unlikely to occur. Most likely, excitation transfer between donors along the direction of the template contributes to energy transfer to the assembly end. Such donor homotransfer of excitations has been observed and modeled for nontemplated, hydrogen-bonded chiral assemblies of conjugated molecules,[4,37] for which it was shown to depend strongly on the extent of order in the assembly. Transfers of this kind may be either dominated again by dipole−dipole coupling between transition moments confined to individual donor chromophores[74] or be of a semi-coherent type, involving delocalization of excitations across more than one donor molecule.[37] Comparison between the simulated and measured energy transfer rates (Table 1) suggests that for the longer ($n \geq 40$) templated assemblies such effects become increasingly significant and therefore need to be included in more comprehensive theoretical modeling.

CONCLUSION

We have investigated energy transfer in a system comprising naphthalene donor chromophores attached via hydrogen bonding to a DNA template decorated with a Cy3.5 acceptor molecule at one end. We find that the efficiency of energy transfer from donor to acceptor depends intricately on temperature and template length, both of which have a strong influence on the extent to which the template is populated with an ordered assembly of donors. Circular dichroism and donor lifetime data show that the assemblies dissociate over a fairly narrow (± 5 °C) temperature range centered around 25 °C. Energy transfer rates decline to zero over the same range as the temperature is raised, indicating that ordered assembly is a prerequisite for energy transfer. In addition, the energy transfer efficiency is found to exhibit a complex dependence on template length, with transfer rates increasing initially with template length toward an optimum for $n = 30$ and then declining again toward $n = 60$. Modeling of the transfer dynamics was carried out with the assumption that Förster transfer occurs between naphthalene donors and Cy3.5 acceptors, whose separations had been determined through molecular modeling, and yielded simulated energy transfer dynamics that are similar in shape to those experimentally measured. The model overestimated real transfer rates at short template lengths for which incomplete or disordered complex assembly is present, which was not included in the model. However, for long templates, the simulation underestimates the measured transfer rates, most likely because the migration

of excitations along the donor assembly contributes significantly to the overall energy transfer process to the end. These results suggest that efficient energy transfer in excess of that expected from simple Förster calculations will be possible even for relatively long DNA-templated assemblies of conjugated chromophores. In summary, our study shows that energy transfer in DNA-templated assemblies is influenced by a number of complex factors. Adoption of these materials for nanoscale sensors and wires thus requires an understanding of the processes that lead to cooperative assembly and order and their influence on the transfer of excitations within these systems.

ASSOCIATED CONTENT

S **Supporting Information.** Additional text, three figures, and one table describing synthesis and characterization of DNA-templated assemblies, extraction of energy transfer dynamics from measured TCSPC PL decay data, and the model describing these transfer dynamics. This material is available free of charge via the Internet at http://pubs.acs.org.

AUTHOR INFORMATION

Corresponding Author
*E-mail l.herz1@physics.ox.ac.uk.

ACKNOWLEDGMENT

REFERENCES

(1) Lehn, J. M.; Mascal, M.; Decian, A.; Fischer, J. *J. Chem. Soc., Chem. Commun.* **1990**, 479–481.

(2) Lehn, J. M.; Rigault, A. *Angew. Chem., Int. Ed. Engl.* **1988**, 27, 1095–1097.

(3) Lehn, J. M.; Rigault, A.; Siegel, J.; Harrowfield, J.; Chevrier, B.; Moras, D. *Proc. Natl. Acad. Sci. U.S.A.* **1987**, 84, 2565–2569.

(4) Chang, M. H.; Hoeben, F. J. M.; Jonkheijm, P.; Schenning, A. P. H. J.; Meijer, E. W.; Silva, C.; Herz, L. M. *Chem. Phys. Lett.* **2006**, 418, 196–201.

(5) Sherwood, G. A.; Cheng, R.; Smith, T. M.; Werner, J. H.; Shreve, A. P.; Peteanu, L. A.; Wildeman, J. *J. Phys. Chem. C* **2009**, 113, 18851–18862.

(6) Spada, G. P.; Lena, S.; Masiero, S.; Pieraccini, S.; Surin, M.; Samor, P. *Adv. Mater.* **2008**, 20, 2433–2438.

(7) Hannah, K. C.; Armitage, B. A. *Acc. Chem. Res.* **2004**, 37, 845–853.

(8) Zhao, Z.; Yan, H.; Liu, Y. *Angew. Chem., Int. Ed.* **2010**, 49, 1414–1417.

(9) Nakamura, M.; Ohtoshi, Y.; Yamana, K. *Chem. Commun.* **2005**, 5163–5165.

(10) Janssen, P. G. A.; van Dongen, J. L. J.; Meijer, E. W.; Schenning, A. P. H. J. *Chem.—Eur. J.* **2009**, 15, 352–360.

(11) Cooper, V. R.; Thonhauser, T.; Puzder, A.; Schröder, E.; Lundqvist, B. I.; Langreth, D. C. *J. Am. Chem. Soc.* **2008**, 130, 1304–1308.

(12) Rothemund, P. W. K. *Nature* **2006**, 440, 297–302.

(13) Dietz, H.; Douglas, S. M.; Shih, W. M. *Science* **2009**, 325, 725–730.

(14) Park, S. H.; Yin, P.; Liu, Y.; Reif, J. H.; Labean, T. H.; Yan, H. *Nano Lett.* **2005**, 5, 729–733.

(15) Pinto, Y. Y.; Le, J. D.; Seeman, N. C.; Musier-Forsyth, K.; Taton, T. A.; Kiehl, R. A. *Nano Lett.* **2005**, 5, 2399–2402.

(16) Mayer-enthart, E.; Wagner, C.; Barbaric, J.; Wagenknecht, H. A. *Tetrahedron* **2007**, *63*, 3434–3439.

(17) Häner, R.; Samain, F.; Malinovskii, V. L. *Chem.—Eur. J.* **2009**, *15*, 5701–5708.

(18) Ueno, Y.; Komatsuzaki, S.; Takasu, K.; Kawai, S.; Kitamura, Y.; Kitade, Y. *Eur. J. Org. Chem.* **2009**, *2009*, 4763–4769.

(19) Iwaura, R.; Hoeben, F. J. M.; Masuda, M.; Schenning, A. P. H. J.; Meijer, E. W.; Shimizu, T. *J. Am. Chem. Soc.* **2006**, *128*, 13298–13304.

(20) Iwaura, R.; Yoshida, K.; Masuda, M.; Ohnishi-kameyama, M.; Yoshida, M.; Shimizu, T. *Angew. Chem., Int. Ed.* **2003**, *42*, 1009–1012.

(21) Janssen, P. G. A.; Brankaert, N. J. M.; Vila, X.; Schenning, A. P. H. J. *Soft Matter* **2010**, *6*, 1494–1502.

(22) Yang, W.; Xia, P. F.; Wong, M. S. *Org. Lett.* **2010**, *12*, 4018–4021.

(23) Shroff, H.; Reinhard, B. M.; Siu, M.; Agarwal, H.; Spakowitz, A.; Liphardt, J. *Nano Lett.* **2005**, *5*, 1509–1514.

(24) Johansson, M. K.; Fidder, H.; Dick, D.; Cook, R. M. *J. Am. Chem. Soc.* **2002**, *124*, 6950–6956.

(25) Sánchez-Mosteiro, G.; van Dijk, E. M. H. P.; Hernando, J.; Heilemann, M.; Tinnefeld, P.; Sauer, M.; Koberlin, F.; Patting, M.; Wahl, M.; Erdmann, R.; van Hulst, N. F.; García-Parajó, M. F. *J. Phys. Chem. B* **2006**, *110*, 26349–26353.

(26) Hannestad, J. K.; Sandin, P.; Albinsson, B. *J. Am. Chem. Soc.* **2008**, *130*, 15889–15895.

(27) Johansson, M. K.; Cook, R. M. *Chem.—Eur. J.* **2003**, *9*, 3466–3471.

(28) Somsen, O. J. G.; Keukens, L. B.; de Keijzer, M. N.; van Hoek, A.; van Amerongen, H. *ChemPhysChem* **2005**, *6*, 1622–1627.

(29) Martí, A. A.; Jockusch, S.; Li, Z. M.; Ju, J. Y.; Turro, N. J. *Nucleic Acids Res.* **2006**, *34*, e50.

(30) Förster, T. H. *Discuss. Faraday Soc.* **1959**, *27*, 7–17.

(31) Lunz, M.; Bradley, A. L.; Chen, W. Y.; Gun'ko, Y. K. *J. Phys. Chem. C* **2009**, *113*, 3084–3088.

(32) Parkinson, P.; Aharon, E.; Chang, M. H.; Dosche, C.; Frey, G. L.; Köhler, A.; Herz, L. M. *Phys. Rev. B* **2007**, *75*, 165206.

(33) Herz, L. M.; Daniel, C.; Silva, C.; Hoeben, F. J. M.; Schenning, A. P. H. J.; Meijer, E. W.; Friend, R. H.; Phillips, R. T. *Phys. Rev. B* **2003**, *68*, 45203.

(34) Maliwal, B. P.; Kuśba, J.; Lakowicz, J. R. *Biopolymers* **1995**, *35*, 245–255.

(35) Chang, M. H.; Frampton, M. J.; Anderson, H. L.; Herz, L. M. *Phys. Rev. Lett.* **2007**, *98*, 27402.

(36) Chang, M. H.; Hoffmann, M.; Anderson, H. L.; Herz, L. M. *J. Am. Chem. Soc.* **2008**, *130*, 10171–10178.

(37) Beljonne, D.; Hennebicq, E.; Daniel, C.; Herz, L. M.; Silva, C.; Scholes, G. D.; Hoeben, F. J. M.; Jonkheijm, P.; Schenning, A. P. H. J.; Meskers, S. C. J.; Phillips, R. T.; Friend, R. H.; Meijer, E. W. *J. Phys. Chem. B* **2005**, *109*, 10594–10604.

(38) Janssen, P. G. A.; Ruiz-Carretero, A.; González-Rodríguez, D.; Meijer, E. W.; Schenning, A. P. H. J. *Angew. Chem., Int. Ed.* **2009**, *48*, 8103–8106.

(39) Ruiz-Carretero, A.; Janssen, P. G. A.; Stevens, A. L.; Surin, M.; Herz, L. M.; Schenning, A. P. H. J. *Chem. Commun.* **2011**, *47*, 884.

(40) Janssen, P. G. A. DNA templated self-assembly. Ph.D. Thesis, Eindhoven University of Technology, Eindhoven, The Netherlands, 2009

(41) Janssen, P. G. A.; Jabbari-farouji, S.; Surin, M.; Vila, X.; Gielen, J. C.; de Greef, T. F. A.; Vos, M. R. J.; Bomans, P. H. H.; Sommerdijk, N. A. J. M.; Christianen, P. C. M.; Leclère, P.; Lazzaroni, R.; van der Schoot, P.; Meijer, E. W.; Schenning, A. P. H. J. *J. Am. Chem. Soc.* **2009**, *131*, 1222–1231.

(42) Janssen, P. G. A.; Vandenbergh, J.; van Dongen, J. L. J.; Meijer, E. W.; Schenning, A. P. H. J. *J. Am. Chem. Soc.* **2007**, *129*, 6078–6079.

(43) Surin, M.; Janssen, P. G. A.; Lazzaroni, R.; Leclère, P.; Meijer, E. W.; Schenning, A. P. H. J. *Adv. Mater.* **2009**, *21*, 1126–1130.

(44) Kasha, M.; Rawls, H. R.; Ashraf El Bayoumi, M. *Pure Appl. Chem.* **1965**, *11*, 371–392.

(45) Harvey, B. J.; Levitus, M. *J. Fluoresc.* **2009**, *19*, 443–448.

(46) Sanborn, M. E.; Connolly, B. K.; Gurunathan, K.; Levitus, M. *J. Phys. Chem. B* **2007**, *111*, 11064–11074.

(47) Torimura, M.; Kurata, S.; Yamada, K.; Yokomaku, T.; Kamagata, Y.; Kanagawa, T.; Kurane, R. *Anal. Sci.* **2001**, *17*, 155–160.

(48) Lv, W.; Chen, X. D.; Aumiler, D.; Xia, A. D. *Sci. China Ser. B: Chem.* **2009**, *52*, 1148–1153.

(49) Iqbal, A.; Arslan, S.; Okumus, B.; Wilson, T. J.; Giraud, G.; Norman, D. G.; Ha, T.; Lilley, D. M. J. *Proc. Natl. Acad. Sci. U.S.A.* **2008**, *105*, 11176–11181.

(50) Levitus, M.; Negri, R. M.; Aramendía, P. F. *J. Phys. Chem.* **1995**, *99*, 14231–14239.

(51) Herz, L. M.; Silva, C.; Friend, R. H.; Phillips, R. T.; Setayesh, S.; Becker, S.; Marsitsky, D.; Müllen, K. *Phys. Rev. B* **2001**, *64*, 195203.

(52) Beljonne, D.; Pourtois, G.; Silva, C.; Hennebicq, E.; Herz, L. M.; Friend, R. H.; Scholes, G. D.; Setayesh, S.; Müllen, K.; Brédas, J. L. *Proc. Natl. Acad. Sci. U.S.A.* **2002**, *99*, 10982–10987.

(53) Herz, L. M.; Silva, C.; Grimsdale, A. C.; Müllen, K.; Phillips, R. T. *Phys. Rev. B* **2004**, *70*, No. 165207.

(54) Berberan-Santos, M. N.; Bodunov, E. N.; Valeur, B. *Chem. Phys.* **2005**, *315*, 171–182.

(55) Baumann, J.; Fayer, M. D. *J. Chem. Phys.* **1986**, *85*, 4087–4107.

(56) Blumen, A.; Manz, J. *J. Chem. Phys.* **1979**, *71*, 4694–4702.

(57) Norman, D. G.; Grainger, R. J.; Uhrín, D.; Lilley, D. M. J. *Biochemistry* **2000**, *39*, 6317–6324.

(58) Pariser, R.; Parr, R. G. *J. Chem. Phys.* **1953**, *21*, 466–471.

(59) Platt, J. R. *J. Chem. Phys.* **1949**, *17*, 484–495.

(60) Klevens, H. B.; Platt, J. R. *J. Chem. Phys.* **1949**, *17*, 470–481.

(61) McClure, D. S. *J. Chem. Phys.* **1954**, *22*, 1668–1675.

(62) Pariser, R. *J. Chem. Phys.* **1956**, *24*, 250–268.

(63) Craig, D. P.; Hollas, J. M.; Redies, M. F.; Wait, S. C. *Philos. Trans. R. Soc. London* **1961**, *253*, 543.

(64) Berden, G.; Meerts, W. L.; Plusquellic, D. F.; Fujita, I.; Pratt, D. W. J. *Chem. Phys.* **1996**, *104*, 3935–3946.

(65) Hashimoto, T.; Nakano, H.; Hirao, K. *J. Chem. Phys.* **1996**, *104*, 6244–6258.

(66) Sony, P.; Shukla, A. *Phys. Rev. B* **2007**, *75*, No. 155208.

(67) Iqbal, A.; Wang, L.; Thompson, K. C.; Lilley, D. M. J.; Norman, D. G. *Biochemistry* **2008**, *47*, 7857–7862.

(68) Ohta, N.; Matsunami, S.; Okazaki, S.; Yamazaki, I. *Langmuir* **1994**, *10*, 3909–3912.

(69) Ranjit, S.; Gurunathan, K.; Levitus, M. *J. Phys. Chem. B* **2009**, *113*, 7861–7866.

(70) Maksimov, M. Z.; Rozman, I. M. *Opt. Spectrosc.* **1961**, *12*, 337–338.

(71) Harvey, B. J.; Perez, C.; Levitus, M. *Photochem. Photobiol. Sci.* **2009**, *8*, 1105–1110.

(72) Schmid, S. A.; Abbel, R.; Schenning, A. P. H. J.; Meijer, E. W.; Herz, L. M. *Phys. Rev. B* **2010**, *81*, No. 085438.

(73) Daniel, C.; Herz, L. M.; Beljonne, D.; Hoeben, F. J. M.; Jonkheijm, P.; Schenning, A. P. H. J.; Meijer, E. W.; Phillips, R. T.; Silva, C. *Synth. Met.* **2004**, *147*, 29–35.

(74) Schmid, S. A.; Abbel, R.; Schenning, A. P. H.; Meijer, E. W.; Sijbesma, R. P.; Herz, L. M. *J. Am. Chem. Soc.* **2009**, *131*, 17696–17704.